

SANDIA REPORT

SAND2019-14890

Printed December 2019



Sandia
National
Laboratories

Method and Apparatus for Semiconductor Defect Characterization

Eric A. Shaner, Ben Olson, Emil Kadlec

Prepared by Eric Shaner
Sandia National Laboratories
Albuquerque, New Mexico
87185 and Livermore,
California 94550

Issued by Sandia National Laboratories, operated for the United States Department of Energy by National Technology & Engineering Solutions of Sandia, LLC.

NOTICE: This report was prepared as an account of work sponsored by an agency of the United States Government. Neither the United States Government, nor any agency thereof, nor any of their employees, nor any of their contractors, subcontractors, or their employees, make any warranty, express or implied, or assume any legal liability or responsibility for the accuracy, completeness, or usefulness of any information, apparatus, product, or process disclosed, or represent that its use would not infringe privately owned rights. Reference herein to any specific commercial product, process, or service by trade name, trademark, manufacturer, or otherwise, does not necessarily constitute or imply its endorsement, recommendation, or favoring by the United States Government, any agency thereof, or any of their contractors or subcontractors. The views and opinions expressed herein do not necessarily state or reflect those of the United States Government, any agency thereof, or any of their contractors.

Printed in the United States of America. This report has been reproduced directly from the best available copy.

Available to DOE and DOE contractors from

U.S. Department of Energy
Office of Scientific and Technical Information
P.O. Box 62
Oak Ridge, TN 37831

Telephone: (865) 576-8401
Facsimile: (865) 576-5728
E-Mail: reports@osti.gov
Online ordering: <http://www.osti.gov/scitech>

Available to the public from

U.S. Department of Commerce
National Technical Information Service
5301 Shawnee Rd
Alexandria, VA 22312

Telephone: (800) 553-6847
Facsimile: (703) 605-6900
E-Mail: orders@ntis.gov
Online order: <https://classic.ntis.gov/help/order-methods/>



ABSTRACT

This report documents efforts to develop a wafer mapping measurement system for semiconductor characterization.

CONTENTS

1. Introduction	9
2. Wafer Mapping Material Properties	10
3. Conclusion	19
4. REFERENCES.....	21

LIST OF FIGURES

Figure 2-1: Schematic (a) top and (b) side views of the carrier lifetime mapper apparatus. The microwave system and excitation laser are both connected to an X-Y translation stage, allowing for them to be scanned over the wafer area.....	14
Figure 2-2: Schematic diagram of the microwave sensor system. This is the same basic system used for both the time-resolved and CW modulated techniques of measuring carrier lifetimes. The signal amplifier before the detector is optional. For the CW technique, the oscilloscope is replaced with a lock-in amplifier.....	15
Figure 2-3: Example focused microwave beam image measured with a Spirocon Pyrocam III beam imager.....	15
Figure 2-4: Minority carrier lifetime map of a 3' photodetector wafer using the time-resolved microwave method. The sample temperature is approximately 150 K (left plot) and 295 K (right plot). Macroscopic non-uniformities can be seen across the wafer, with the center displaying slightly shorter lifetimes than the edges.....	16
Figure 2-5: Carrier lifetime decays using the time-resolved microwave system on 3 narrow-bandgap infrared photodetectors, where (a) is an undoped photodetector, (b) is an with the absorber doped at $1\text{E}15\text{ cm}^{-3}$, and (c) is an photodetector with the absorber doped at $1\text{E}16\text{ cm}^{-3}$. The insets to each figure are the maximum time-resolved microwave reflectance signal (TMR), found shortly after zero time delay, as a function of the particular injected carrier density.....	16
Figure 2-6: Transformed data from Fig. 2-5 showing carrier lifetimes as a function of excess carrier density. The SRH, radiative, and Auger components have been distinguished and are plotted individually. The approximate doping level has also been determined and is located at the elbow in the curve at which the lifetimes level off and become constant with excess carrier density.....	17
Figure 2-7: Modulated CW microwave data to measure carrier lifetimes in a photodetector structure. The sample is excited with a sine-wave modulated CW laser and the resulting carrier density modulation read out using the microwave sensor and a lock-in amplifier. This signal amplitude is then monitored as a function of modulation frequency and the lifetime determined by the -3db roll off frequency [1]. Various pump powers were used to demonstrate the sensitivity of the approach.....	17
Figure 2-8: Photoluminescence measurements. (a) Similar measurement geometry is used for PL mapping and lifetime mapping. Light collected by a paraboloid is sent to a spectrometer such as a FTIR for processing. (b) X and Y motion of the paraboloid and an accompanying steering mirror allow for guiding of light to the spectrometer.....	18

This page left blank

ACRONYMS AND DEFINITIONS

Abbreviation	Definition
IR	Infrared
PL	Photoluminescence
TMR	Time-resolved Microwave
TRPL	Time-resolved photoluminescence
CW	Continuous wave

1. INTRODUCTION

Cryogenic wafer mapping the material properties of epitaxial device wafers arose from the internal need to prescreen infrared (IR) photodetector device wafers before the commitment is made to fabricate the wafers into devices. Wafer mapping has also proved helpful in diagnosing general crystal growth issues. The most useful characterizations are to nondestructively measure the minority carrier lifetime and photoluminescence spectrum of the IR absorbing layer in the photodetector structure at relevant temperatures. The minority carrier lifetime is the characteristic recombination time for excess charge at a density far below the background doping density of the material. The importance of the carrier lifetime for photodetectors is summarized by Eq. 1,

$$\text{Eq. 1: } J_{diff} = q_e \frac{n_i^2 L_{abs}}{N_d \tau}$$

where J_{diff} is the photodetector diffusion current in the dark, q_e is the electronic charge, n_i is the intrinsic carrier density, L_{abs} is the length of the absorber layer, N_d is the absorber doping density, and τ is the minority carrier lifetime [1].

Ideally, a photodetector's dark current is limited by diffusion current and τ is the only parameter that is impacted by the material quality of the absorber and other epitaxial growth layers. The rest of the governing terms in Eq. 1 are set either by intrinsic material properties (i.e. n_i), to meet a specific performance metric (i.e. L_{abs} in terms of quantum efficiency), or by growth conditions (N_d). Minority carrier lifetime is therefore one of the most critical parameters that directly determine the photodetector dark current and subsequently the end performance of the photodetector or focal plane array and the maximum allowable operating temperature for competitive performance.

2. WAFER MAPPING MATERIAL PROPERTIES

We have designed and implemented an apparatus and analysis method to accurately and quickly spatially map the minority carrier lifetime, and other material parameters, over the entire useful area of pre-processed photodetector wafers at cryogenic temperatures. Performing measurements at cryogenic temperatures is important since IR detectors require cooling to temperatures below 150K to operate. The measurement system and methods described here are nondestructive in that they do not require any processing of the wafer or harm the wafer in any way. This approach allows for performance estimation and wafer screening to be done prior to incurring the labor and cost associated with processing and hybridization into a focal plane array.

The basic “wafer mapper” is shown schematically in Figure 2-1. A semiconductor wafer is placed on top of a metal wafer chuck that has internal flow-through lines for liquid nitrogen. It is common practice to apply vacuum grease between a semiconductor sample and cryogenic sample holder (wafer chuck) to create a thermal link. However, this would be detrimental to the wafer as grease is difficult to remove and could create problems with future processing. To avoid this complication, we currently use a sheet of indium foil between the wafer and wafer chuck and mechanically clamp the wafer perimeter to the chuck to create thermal contact. The indium foil leaves no residue on the wafer and does not affect subsequent fabrication processes. Using cryogenic flow-through allows us to cool the wafer chuck from 300 K to 77 K in approximately 30 minutes. Currently, it takes approximately 45 minutes to 60 minutes to map a 3 inch diameter wafer and another 60 minutes to warm the wafer chuck back to room temperature. This allows for a wafer to be mapped at a rate of 1 wafer every 3 hours. A heater installed in the wafer chuck allows for temperature tuning in the 77 K to 300 K range. Similar performance can be obtained using a closed cycle cooling system for cryogen free operation. Our system is also amenable to larger wafer sizes. Due to the point scanning nature of the measurement system, the primary requirement for larger wafers is a suitably sized wafer chuck and optical window, as well as X-Y motorized translation stages with long enough travel to meet the wafer diameter requirements, all of which are readily available from commercial vendors.

For time-resolved carrier lifetime characterization, a fiber coupled pulsed laser is used to inject charge carriers into the absorber layer of the photodetector wafer over an area determined by the spot size of the laser focus at the wafer plane. The spot size for the wafer maps presented in this report is 4 mm and a 1064 nm YAG laser operating at a repetition rate of 1 kHz and pulse widths of approximately 3 ns is used as the excitation source. The system also allows for different wavelengths to be used for the pulsed laser and a tunable laser could be used to allow excitation of particular device layers. While not required, for convenience the laser should be fiber coupled and recent developments in commercially available fiber allow fiber coupling of pump sources out to 12 microns. The decay of excited carriers back to equilibrium, the time scale of which is the carrier lifetime, is measured using a microwave system that is sensitive to changes in conductivity in the excitation area. This change in conductivity is directly correlated to the excess carrier density injected by the laser.

The microwave system is shown schematically in Figure 2-2. Microwaves are sourced by a 95 GHz Gunn diode and directed through a circulator towards the wafer surface using a microwave horn. Any reflected microwaves from the sample are sent via the circulator to a fast microwave detector such as a zero bias Schottky diode or zero bias GaAs beam lead diode. The Gunn diode

has approximately 5 GHz of wavelength tuning via an external voltage that is used to impedance match with the wafer sample and maximize the reflected signal amplitude. The microwave frequency employed for measurements is not critical so long as it is sufficiently low that microwave reflection can be altered by injected charge.

Other than the cryostat window, there are no optics between the microwave horn and wafer surface in the system reported here, however, optics to collimate and focus the microwave beam can be implemented to boost sensitivity (TPX lenses, Teflon lenses, parabolic mirrors, or a combination of these). Additional microwave optics can also allow for greater working distance and normal incidence laser delivery as opposed to the off-normal delivery shown in Figure 2-1. An example microwave beam image through a corrected Gaussian microwave optic is shown in Figure 2-3.

The transient reflected microwave response to pulsed laser excitation of the wafer is acquired from the microwave detector using a wide bandwidth voltage preamplifier and a 12-bit resolution oscilloscope. A wide range of preamps and digitizers could be used for this purpose, we have just found in general using 12-bit or higher resolution provides good results when combined with ~ 40 dB preamp gain. The microwave sensor head and laser source are attached to an X-Y translation stage system that allows for them to be scanned over the wafer area. The microwave reflection approach is bandgap insensitive, we have been able to measure carrier lifetimes on materials with bandgap energies from $1.7 \mu\text{m}$ to $18 \mu\text{m}$. Thus far we have been unable to find an IR material that our system is incapable of measuring. Representative lifetime wafer maps from the system are shown in Figure 2-4.

For our purposes, the microwave reflectance approach is orders of magnitude more sensitive than other methods that can be used to measure carrier lifetimes of narrow bandgap heterostructures such as time-resolved photoluminescence (TRPL) [2] and time-resolved pump-probe [3]. A metric to quantify this is the excited carrier density that the particular method can resolve. For instance, time-resolved photoluminescence is typically good down to carrier densities of 10^{14} cm^{-3} in IR materials of conventional thickness (less than 10 microns). Time-resolved pump-probe methods have similar limits. To reach these sensitivities, it is common to average over 10's of minutes or even hours to recover a single decay curve. In comparison, our microwave system can resolve excited carrier densities in typical absorber thicknesses down to 10^{12} cm^{-3} in a matter of seconds to minutes. This sensitivity increase allows for lifetimes to be determined very quickly, thereby allowing for the mapping of large wafers in a time-frame that is practical for production level growth firms. The microwave reflectance approach does not require that the material being tested can emit light as is required for PL based methods, which can be an additional advantage when troubleshooting growth issues. A disadvantage of TRPL characterization for high-quality materials is that this method becomes less effective as material quality improves. The requirement to operate in the low-injection regime for minority carrier lifetime measurements fixes the amount of charge that can be generated for excitation. As materials improve and lifetimes increase, the photon emission rate decreases leading to reduced signal reaching the PL detector. Microwave based interrogation is immune to this effect as it measures charge in the sample as opposed to photons being emitted.

We utilize two methods for time-resolved lifetime characterization. The simplest approach is to reduce the pulsed laser pump power to a low enough level that low-injection conditions are met.

In this case, a single exponential decay will normally be observed with the characteristic time being the minority carrier lifetime. Typically, 1000 to 10000 captures are averaged to obtain adequate signal-to-noise. As previously stated, the spatial resolution is defined by the excitation spot size of the laser and not the flood area of microwaves. The tail end of the decay curve is then fit with an exponential decay function to extract the minority carrier lifetime. The low-injection excitation power and tail-end fitting procedure ensure that the extracted lifetime is representative of the minority carrier lifetime.

Another method that we use, which provides more information about the structure, requires operation in the high-injection regime (injected carrier density greater than the background doping level) and calibration of the microwave response. To begin, carrier lifetime decay rates at a single interrogation area are recovered for multiple pump powers, and hence injected carrier densities. An example of this is shown in Figure 2-5. The maximum pulsed response is obtained at each power level and a plot such as the insets to Figure 2-5 is made. These data are fit to a phenomenological function and allow for us to determine, based on how much signal there is at any particular delay time, the excess carrier density present. This result is a transfer function that maps signal amplitude to excess carrier density. The raw time-resolved data are transformed into instantaneous carrier lifetimes (τ) as a function of excess carrier density using [4],

$$\text{Eq. 2: } \tau^{-1} = -\frac{1}{\Delta n} \frac{\partial \Delta n}{\partial t} = -\frac{1}{\Delta n} \frac{\partial \Delta n}{\partial S} \frac{\partial S}{\partial t}$$

where Δn is the excess carrier density and S is the microwave signal. The $\partial \Delta n / \partial S$ term is determined from the inset to Figure 2-5 and the $\partial S / \partial t$ term is determined from the decay curves in Figure 2-5. These data provide more information than a single lifetime constant since it probes both high and low injection regimes (i.e. excess carrier densities both above and below the absorber doping level). This is important since the measured lifetime is a convolution of three different carrier recombination mechanisms and the relative importance of these mechanisms depend on injection level. These are Shockley-Read-Hall (defect mitigated), radiative, and Auger (energy transferred to third charge carrier) recombination. In general, the total lifetime is,

$$\tau^{-1} = \tau_{SRH}^{-1} + \tau_{rad}^{-1} + \tau_{auger}^{-1}$$

By analyzing our time-resolved data in the manner described above, we have developed a method to differentiate these three mechanisms from the measured lifetime. This is possible because 1) we include a doping level in the analysis and 2) our lifetime data encompasses 4-5 orders of magnitude in excess carrier density. From this analysis method, we can ascertain not just the minority carrier lifetime, but also the Shockley-Read-Hall defect lifetimes, the radiative lifetime and coefficient, the Auger lifetime and coefficient [5], and the doping level [6] as a function of position on a semiconductor wafer. An example of the advanced analysis that is possible is shown in Figure 2-6.

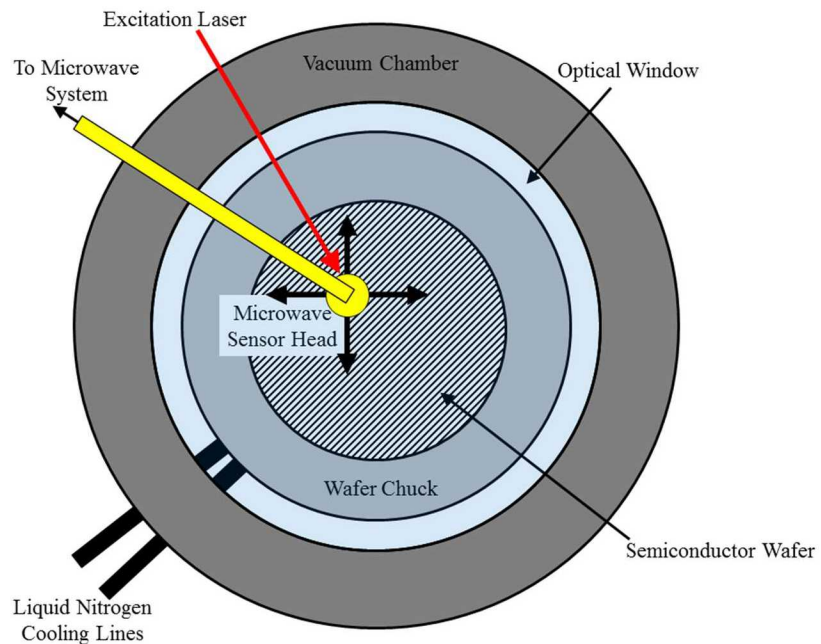
It should be noted that there are additional requirements for this more complex approach to be valid. One is that a spatially uniform pumping must be implemented. In practice, this is often accomplished by expanding the pump beam to have a relatively flat power distribution across the microwave probe area. In addition, the absorber should be pumped using a wavelength close to the band edge to ensure relatively uniform carrier density generation in the region of interest. Finally, for carrier density calibration to be accurate, the absorption coefficient at the pump

wavelength must be known [5]. Deviations from uniform pump conditions will introduce errors into the analysis that is difficult to quantify without more complex transport modeling.

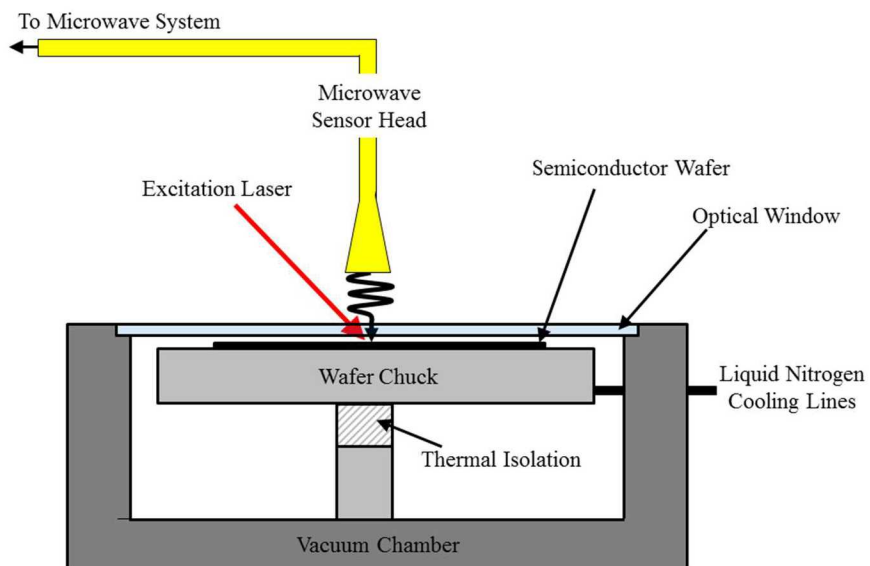
Besides time-resolved recovery of the carrier lifetime, we have also developed a modulated continuous wave technique using the same microwave system and sensor head [2]. This technique involves using a widely available CW telecom laser ($1.55\text{ }\mu\text{m}$ wavelength) as the excitation source instead of a pulsed laser. The CW laser intensity is modulated slightly by a sine wave signal at a particular frequency and the resulting carrier density fluctuations are read out using the microwave sensor. The use of a lockin amplifier to analyze the microwave signal instead of an oscilloscope allows measurements of even lower carrier density signals due to the lockin amplifier's superior noise reduction. To perform measurements, the modulation frequency is swept from low to high frequencies. When the modulation frequency is greater than the carrier recombination rate, the excess carriers can no longer follow the intensity modulation and the signal amplitude at the carrier frequency decreases. The carrier lifetime is then determined by the -3db roll-off frequency. Sensitivities down to 10^{11} cm^{-3} have been demonstrated using this approach. Examples of modulated CW lifetime extraction are shown in Figure 2-7. This method may allow for increased speed in recovery of the minority carrier lifetime, which would be useful for larger area wafers. However, in our opinion, sweeping the modulation frequency of a laser adds complexity that may not be practical for wafer mapping in general. It should be noted that it is also possible to obtain lifetime information through phase shift analysis as opposed to monitoring the amplitude [7].

Another option for increased sensitivity and measurement speed is heterodyne detection of the microwave signal. This approach would use a similar general setup as described for pulsed measurements and would work for both the time-resolved and modulated CW microwave techniques. A heterodyne approach would require that the microwave detector be replaced by a mixer as well as a second microwave source (or derived frequency) to serve as a local oscillator to mix with the return signal. Due to the $\sim 100\text{ GHz}$ carrier frequency being significantly higher than any Fourier components of the lifetime responses (1 GHz max), in principle heterodyne detection and its related filtering benefits could be reasonably employed.

The bandgap of the as-grown material is also an important material property relevant to growth characterization. A simple scanning mirror system shown in Figure 2-8 allows for photoluminescence (PL) light collection to be performed using the same cryosystem described in this report. This PL mapping measurement arrangement is the same as a typical single point PL measurement except that the collection paraboloid and excitation laser scan in the X and Y directions. This motion is matched to a steering mirror that has motion in the Y direction. The resulting collected light is sent to a spectrometer such as a Fourier transform infrared spectrometer (FTIR) for processing.



(a)



(b)

Figure 2-1: Schematic (a) top and (b) side views of the carrier lifetime mapper apparatus. The microwave system and excitation laser are both connected to an X-Y translation stage, allowing for them to be scanned over the wafer area.

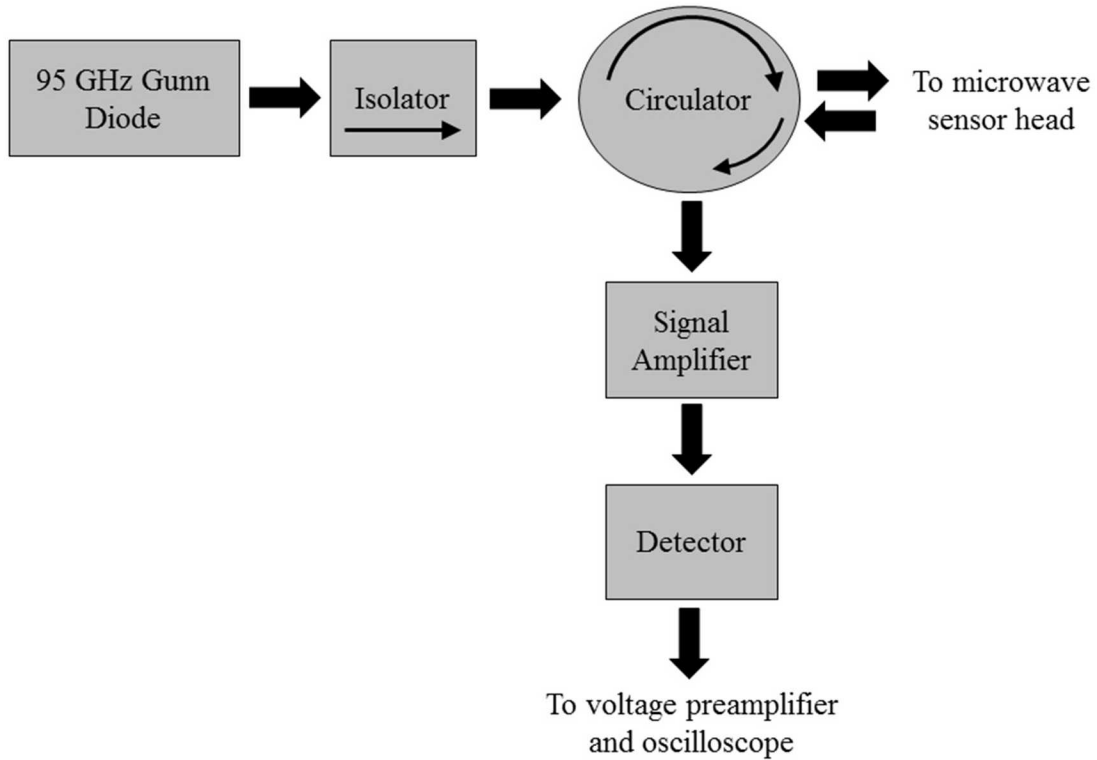


Figure 2-2: Schematic diagram of the microwave sensor system. This is the same basic system used for both the time-resolved and CW modulated techniques of measuring carrier lifetimes. The signal amplifier before the detector is optional. For the CW technique, the oscilloscope is replaced with a lock-in amplifier.

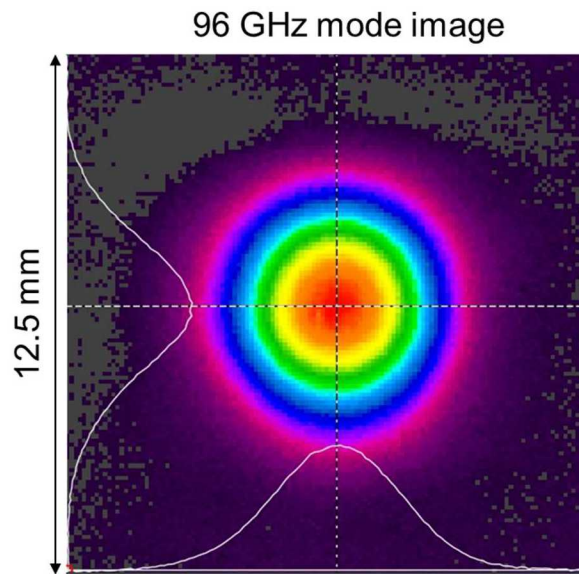


Figure 2-3: Example focused microwave beam image measured with a Spirocon Pyrocam III beam imager.

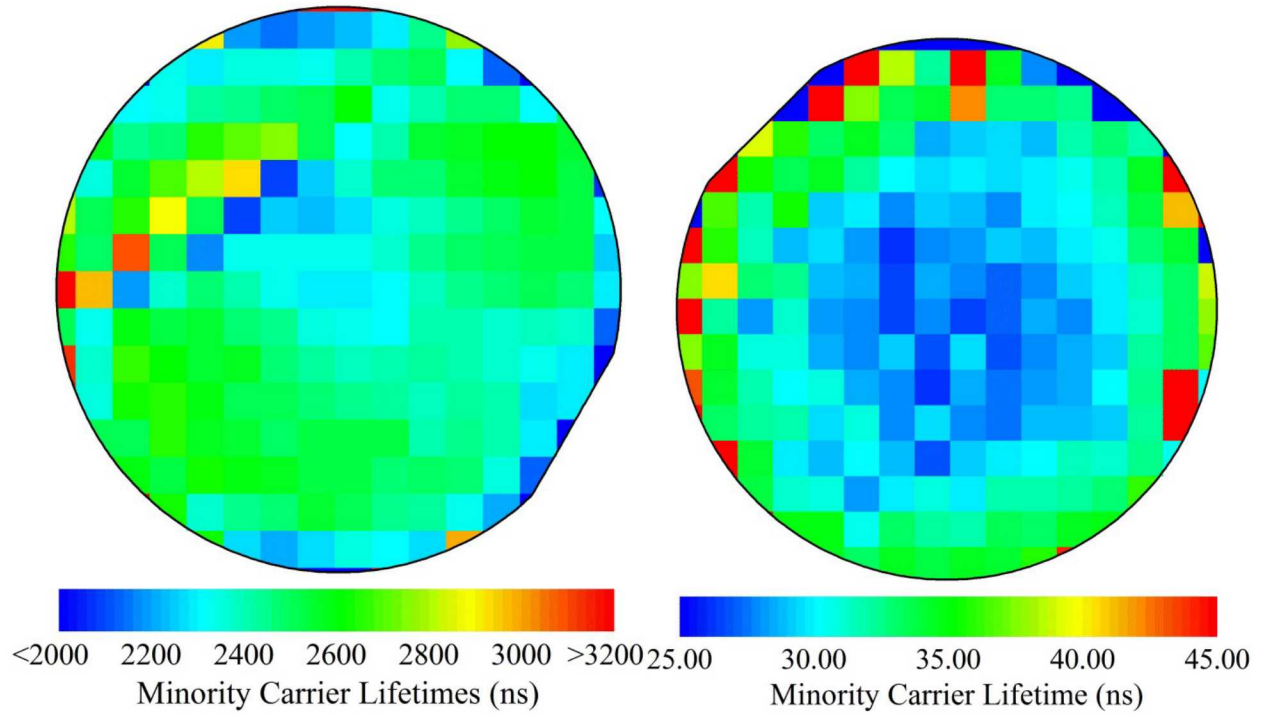


Figure 2-4: Minority carrier lifetime map of a 3' photodetector wafer using the time-resolved microwave method. The sample temperature is approximately 150 K (left plot) and 295 K (right plot). Macroscopic non-uniformities can be seen across the wafer, with the center displaying slightly shorter lifetimes than the edges.

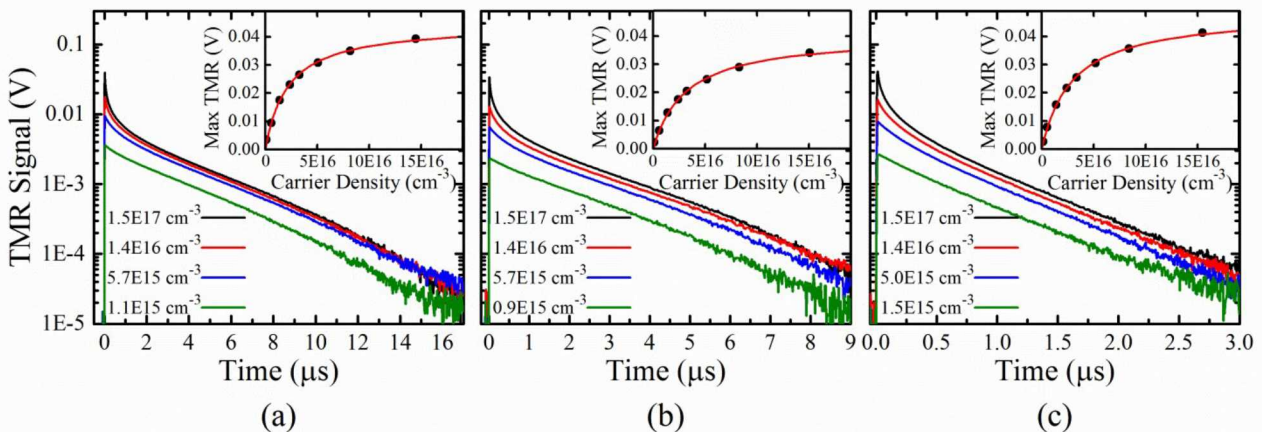


Figure 2-5: Carrier lifetime decays using the time-resolved microwave system on 3 narrow-bandgap infrared photodetectors, where (a) is an undoped photodetector, (b) is an with the absorber doped at $1\text{E}15\text{ cm}^{-3}$, and (c) is an photodetector with the absorber doped at $1\text{E}16\text{ cm}^{-3}$. The insets to each figure are the maximum time-resolved microwave reflectance signal (TMR), found shortly after zero time delay, as a function of the particular injected carrier density.

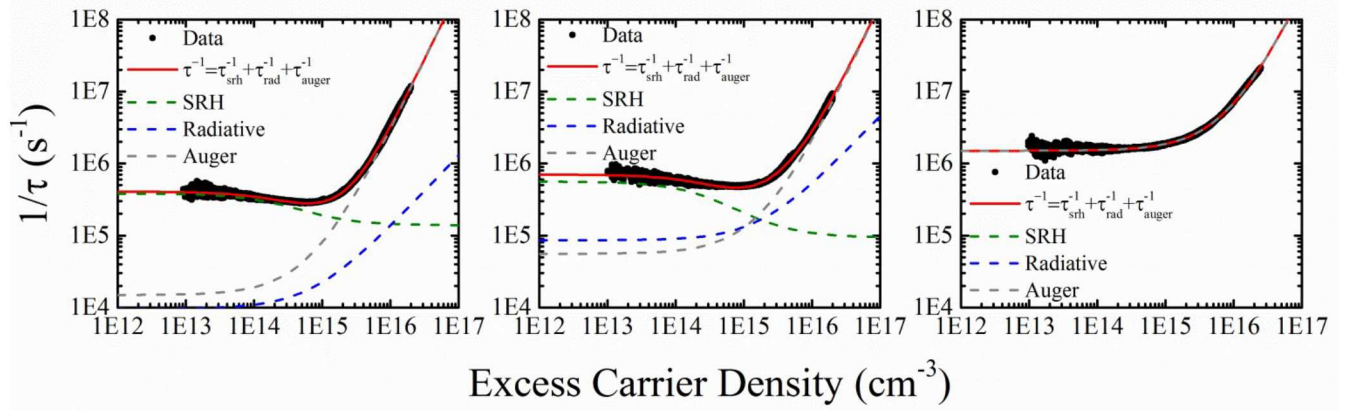


Figure 2-6: Transformed data from Fig. 2-5 showing carrier lifetimes as a function of excess carrier density. The SRH, radiative, and Auger components have been distinguished and are plotted individually. The approximate doping level has also been determined and is located at the elbow in the curve at which the lifetimes level off and become constant with excess carrier density.

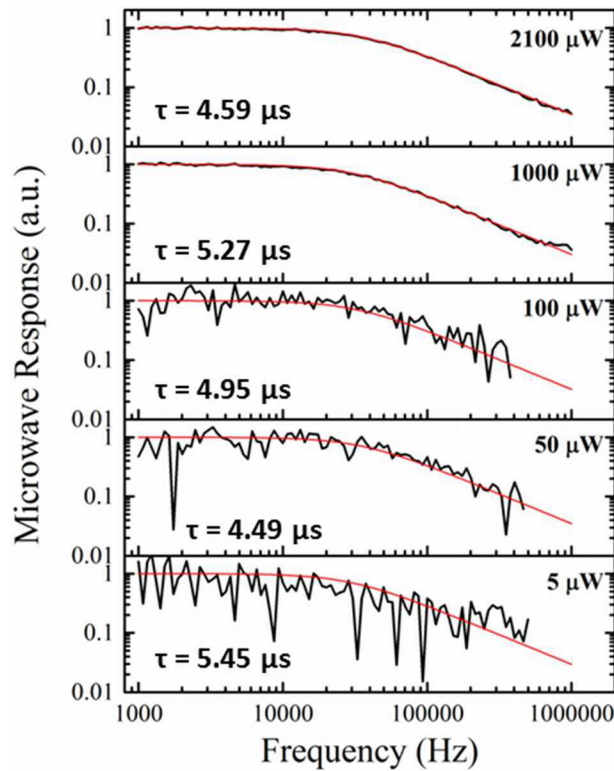


Figure 2-7: Modulated CW microwave data to measure carrier lifetimes in a photodetector structure. The sample is excited with a sine-wave modulated CW laser and the resulting carrier density modulation read out using the microwave sensor and a lock-in amplifier. This signal amplitude is then monitored as a function of modulation frequency and the lifetime determined by the -3db roll off frequency [1]. Various pump powers were used to demonstrate the sensitivity of the approach.

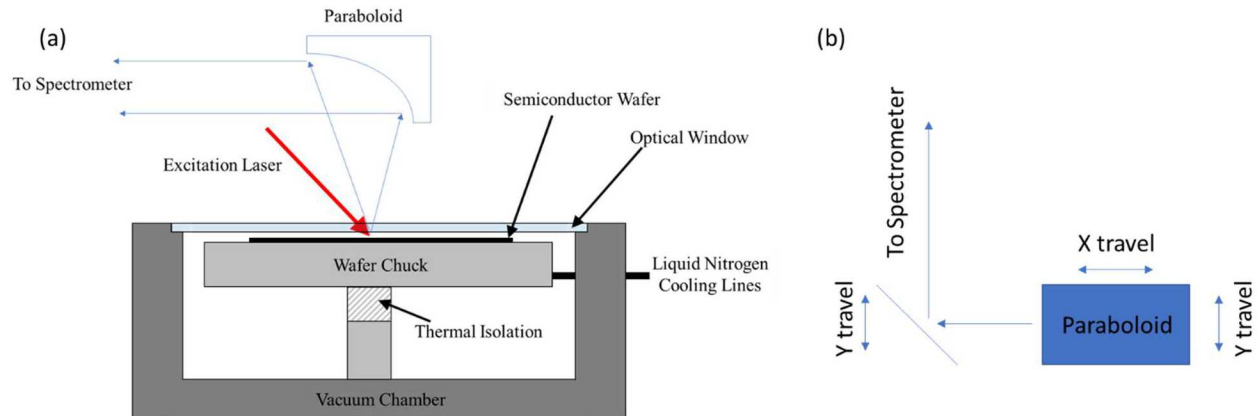


Figure 2-8: Photoluminescence measurements. (a) Similar measurement geometry is used for PL mapping and lifetime mapping. Light collected by a paraboloid is sent to a spectrometer such as a FTIR for processing. (b) X and Y motion of the paraboloid and an accompanying steering mirror allow for guiding of light to the spectrometer.

3. CONCLUSION

This work documents the basic principles of a cryogenic material characterization system intended for nondestructive measurements of as-grown semiconductor wafers. All measurements are performed using a scanning single-point measurement head. Analysis approaches were described that allow extraction of relevant material properties from the acquired data. While the single-point scanning nature of the system requires significant measurement time, the availability of closed cycle refrigerators offer turn-key options for data acquisition. We have found this wafer mapping approach to be useful for verifying material quality and diagnosing growth issues.

4. REFERENCES

- [1] D. R. Rhiger, Performance Comparison of Long-Wavelength Infrared Type II Superlattice Devices with HgCdTe, *J. Electron. Mat.*, 40, 1815–1822 (2011)
- [2] Kadlec, Emil A., "Progress Towards Competitive III-V Infrared Detectors: Fundamental Material Characterization and Techniques." (2017). https://digitalrepository.unm.edu/ece_etds/359
- [3] B.V. Olson, E.A. Shaner, J.K. Kim, J.F. Klem, S.D. Hawkins, L.M. Murray, J.P. Prineas, M.E. Flatté, T.F. Boggess, Time-resolved optical measurements of minority carrier recombination in a mid-wave infrared InAsSb alloy and InAs/InAsSb superlattice, *Appl. Phys. Lett.* 101, 092109 (2012).
- [4] M. E. Flatté, C. H. Grein, T. C. Hasenberg, S. A. Anson, D. J. Jang, J. T. Olesberg, and T. F. Boggess, Carrier recombination rates in narrow-gap InAs/Ga_{1-x}In_xSb-based superlattices, *Phys. Rev. B* 59, 5745 (1999).
- [5] B. V. Olson, E. A. Kadlec, J. K. Kim, J. F. Klem, S. D. Hawkins, E. A. Shaner, and M. E. Flatté, Intensity- and Temperature-Dependent Carrier Recombination in InAs/InAs_{1-x}Sb_x Type-II Superlattices, *Phys. Rev. Applied* 3, 044010 (2015).
- [6] E. A. Kadlec, B. V. Olson, M. D. Goldflam, J. K. Kim, J. F. Klem, S. D. Hawkins, W. T. Coon, M. A. Cavalieri, A. Tauke-Pedretti, T. R. Fortune, C. T. Harris, and E. A. Shaner, Effects of electron doping level on minority carrier lifetimes in n-type mid-wave infrared InAs/InAs_{1-x}Sb_x type-II superlattices, *Appl. Phys. Lett.* 109, 261105 (2016).
- [7] M.S. Ridout, Measurement of Minority Carrier Lifetime by the Phase Shift of Photoconductivity. In: Schön M., Welker H. (eds) Halbleiter und Phosphore / Semiconductors and Phosphors / Semiconducteurs et Phosphores. Vieweg+Teubner Verlag, Wiesbaden, https://doi.org/10.1007/978-3-663-02557-3_36 (1958)

Distribution

Email—Internal

Name	Org.	Sandia Email Address
Technical Library	01977	sanddocs@sandia.gov

This page left blank

This page left blank



**Sandia
National
Laboratories**

Sandia National Laboratories is a multimission laboratory managed and operated by National Technology & Engineering Solutions of Sandia LLC, a wholly owned subsidiary of Honeywell International Inc. for the U.S. Department of Energy's National Nuclear Security Administration under contract DE-NA0003525.